

1 **Transcriptional analysis of the *dachsous* gene uncovers novel isoforms expressed**
2 **during development**

3

4 Eva Revilla-Yates^{1*}, Laura Varas^{1*}, Javier Sierra² and Isabel Rodriguez^{1,3}

5

6 1 Centro de Biología Molecular “Severo Ochoa”. Nicolas Cabrera, 1. Campus Cantoblanco.
7 28049 - Madrid. Spain.

8 2 Departamento de Biotecnología. Universidad Francisco de Vitoria. 28223 - Pozuelo de
9 Alarcón. Madrid. Spain.

10 3 Correspondence to: isabel.rodriguez@mineco.es

11 * These authors contributed equally to this work.

12

13

14

15

16

17

18

19

20

21

22

23

24

25

26

27

28

29 **ABSTRACT**

30 The *Drosophila* cadherin-related protein Dachsoous (Ds) plays a prominent role in planar cell
31 polarity (PCP) and growth. The regulation of these two processes is based on the interaction
32 between Ds and Fat proteins, generating an intracellular response required for tissue
33 polarization and modulation of Hippo pathway activity. Here we have performed a
34 comprehensive molecular study of the *ds* gene during larval development that has shown an
35 unexpected complexity in its transcriptional regulation and revealed the expression of
36 hitherto unsuspected transcripts. Also, knockdown of several isoforms provides new
37 evidence on the importance of the cytoplasmic domain in the mechanism of action of Ds
38 during development.

39

40

41 **KEYWORDS:** *Drosophila* / growth / PCP/ Dachsoous transcripts / DsIntra isoform.

1 **HIGHLIGHTS**

- 2 • Three novel transcriptional isoforms of *dsgene* are expressed during larval
3 development.
- 4 • The cytoplasmic domain of *Ds* plays an essential role in control growth and PCP.
- 5 • *Ds* regulates the mitochondrial activity.

1 INTRODUCTION

2 Numerous tissues undergo an additional level of organization through an
3 evolutionary conserved mechanism called planar cell polarity (PCP), which contributes to
4 the development of fully functional organs of a precise size and shape. The *Drosophila*
5 cadherin-related Dachsous (Ds) and Fat (Ft) proteins and their homologues in vertebrates,
6 participate in the control of PCP and growth (reviewed in [1]). The current model is based
7 on the heterophilic interaction between these two single-pass transmembrane proteins. This
8 interaction generates a signaling cascade mediated by the Ft intracellular domain and
9 resulting in cytoskeletal reorganization and modulation of the Hippo pathway [2, 3].

10 During *Drosophila* wing formation, Ds regulates different processes such as the
11 orientation of cell division, specification of proximal-distal (P/D) patterning, vein formation
12 and wing hairs orientation [4-6]. Thus, herein the term PCP/patterning will be used to
13 encompass all these PCP processes.

14 In addition, Ds can control tissue growth, modulating the activity of Hippo signalling
15 pathway. This role of Ds is related to its ability to regulate the expression of genes such as
16 *four jointed (fj)* [7] and *dally* and *dally-like (dlp)*, key modulators of the Hedgehog, Wnt and
17 TGF- β signalling pathways involved in cell proliferation and patterning [8];[9].

18 Significant progress has been made in understanding the mechanism by which Ft
19 regulates PCP and growth, due to the identification of cytoplasmic partners that interact with
20 specific sequence motifs of Ft cytoplasmic domain (CD) [10-13]. However, less understood
21 is the molecular mechanism of Ds regulating PCP and Hippo pathway. Reported data
22 provide genetic evidence that Ds can regulate these processes in two different ways: cell-
23 autonomous and non-cell autonomous manner. Therefore, PCP and growth can be also
24 regulated by Ds independently of Ft [7, 8, 14, 15]. At present, it is difficult to envision how
25 the current model, based on the requirement of the extracellular domain of Ds, can explain
26 the cell-autonomous function.

27 In this work, the molecular analysis of the *ds* gene reveals the expression of several
28 *ds* transcriptional variants in imaginal discs and brain during larval development. We have

29 characterized three novel isoforms that encode the soluble proteins DsEx, Ds1 and DsIntra.
30 Moreover, we show that the cytoplasmic isoforms can regulate not only PCP/patterning and
31 growth but also mitochondrial activity, indicating a relevant role of the cytoplasmic domain in
32 the mechanism of action of Ds during development.

33

34 MATERIALS AND METHODS

35 *Drosophila* genetics

36 *ds* mutant alleles *ds*¹, *30AG4* and *ds*^{38k}, and the Gal4 lines *638-Gal4*, *en-Gal4*, *hh-Gal4* and
37 *tub-Gal4*, were obtained from the Bloomington Stock Center. *puc-lacZ* (*puc*^{E69}; [16]). RNAi
38 lines were obtained from VDRC (<http://stockcenter.vdrc.at/control/main>). *ds*¹ and *30AG4* are
39 weak alleles caused by transposable elements inserted in coding exons of the extracellular
40 domain [17]. *ds*^{38k} is a spontaneous mutation not affecting the coding exons (our
41 sequencing analysis). In turn, *ds*^{36D} is a strong allele generated by P-excision of *ds*⁰⁵¹⁴² [5].
42 UAS-DsFL [18] comprises the complete coding region of full-length Ds [17]. UAS-ectoDs
43 encodes a large extracellular domain anchored to the cell membrane [15]. The UAS-
44 DsIntraV5 transgene was generated by fusion of the cDNA sequence (nt 10153 to 11464;
45 Genbank: L08811.2) and one copy of V5 epitope to the C-terminus (Ct) in the pUAS-T
46 vector. The UAS-DsExGFP transgene comprises from exon2 to exon10 (nt 796 to 6832;
47 Genbank: L08811.2) and one copy of GFP sequence joined to the 3' end of exon10. The aa
48 sequences of the fusion are: UAS-DsIntraV5 ...GTRMSRGPFE**GKPIP**N... and UAS-
49 DsExGFP ...LITTVGAGTMVSKGE... (*ds* sequences are underlined and V5 and GFP
50 sequences appear in boldface). To analyze wing phenotypes, the transgenes *dsRNAi-cyt*,
51 *dsRNAi-ex*, DsFL, UAS-ectoDs, DsExGFP and DsIntraV5 were overexpressed in a wild-
52 type (wt) background under the control of *638G4*, *enG4* and *hhG4* drivers. For
53 quantitation, the A-PCV and wing area between 4 and 12 wings of each genotype were
54 traced using Adobe Photoshop CS3. The average of distance and area was normalized to
55 control females. Measurement of A-PCV distance was made as described in [11]. The wing

56 area parameter was calculated dividing the posterior area(P)by the total area (T) (Figure
57 S1).

58

59 **Statistical analysis**

60 In all the experiments, significance was determined using the Student's t-distribution (two
61 tailed; two sample equal variances). A *p*value of <0.05 was considered statistically
62 significant.

63

64 **Immunohistochemistry**

65 Wing imaginal discs were dissected and stained as described in [19]. Primary antibodies
66 used for histology were: rabbit anti-Dachsous (Ds^{ex} 1:1000 [20], guinea pig anti-Dachsous
67 (Ds^{cyt} 1:500; this work), mouse anti-COXIV (1:50; Invitrogen), rabbit anti-β-galactosidase
68 (1:10000; Cappel), rabbit anti-Caspase 3 (1:200, Cell Signalling), mouse anti-Dlp (1:100;
69 Developmental Studies Hybridoma Bank)and mouse anti-V5 (1:2000; Invitrogen).Proteins
70 were visualized using fluorescent secondary antibodies (Jackson ImmunoResearch
71 Laboratories).Analysis of Ds expression in mitochondriawas determined by co-
72 immunostaining in fat body cells of third instar larvae [21]. ROS production was evaluated in
73 live tissues using Dihydroethidium (DHE), the *Drosophila*imaginal discs were dissected
74 following the protocol described in [22].The guinea pig Ds antibody against the cytoplasmic
75 region was generated from a GST fusion protein (pGEX4T2 vector) containing the amino
76 acids 3410-3700 (AAF51468.3). Imaginal discs were mounted in Vectashield (Vector
77 Laboratories) and Mowiol. Images were acquired using a Zeiss Confocal LSM510
78 microscope.

79

80 **Quantitative real-time PCR and data analysis**

81 Total RNA was extracted from three independent biological samples (imaginal discs and
82 brains) of wt and *tubG4/UAS-dsRNAi* larvaeto determine the expression of individual exons
83 by two-step real-time PCR (RT-PCR). The first strand cDNA was synthesized with the

84 Transcriptor First Strand cDNA Synthesis kit (Roche) using 2 µg of total RNA and oligo(dT)
85 primer. For the second step of qRT-PCR amplification, a pair of primers for each coding
86 exon was designed following the recommendations of the Universal Probe Library Assay
87 Design Center (Roche Applied Science). The *Tbp* and *eIF-2α* genes were used as
88 endogenous controls for analysis of RNA quantity and quality. Primer sequences and
89 amplicon size are indicated in Table S1. All PCR reactions were carried out in technical
90 duplicates using HotStart Taq polymerase (Qiagen) and SYBR green (Qiagen) in an optical
91 384-well plate with ABI 7900HT (Applied BioSystems). For absolute quantification (standard
92 curve method), the *pUAS-dsFL* (exons 2-12) construct was used as standard [18] (Table
93 S2). For the standard curves, 5 serial 10-fold dilutions from the same reaction mixture of
94 *pUAS-ds* were amplified. For relative quantification, the normalization of different biological
95 samples was performed using the comparative Ct ($2^{-\Delta\Delta Ct}$) method after efficiency calculation
96 for each primer pair (Table S3). For statistical analysis of the experimental groups,
97 differences in mean values were analyzed with the one-tailed nonparametric Student t-test.
98 A p-value <0.05 was considered statistically significant. Data analysis was carried out using
99 Integromics RealTime StatMiner software (<http://www.integromics.com/StatMiner>).

100

101 **Analysis of RACE products**

102 cDNA libraries were obtained with the SMARTer RACE (rapid amplification of cDNA ends)
103 cDNA amplification kit (Clontech) from two independent biological samples of total RNA of
104 wt imaginal discs and brains. PCR amplification was performed with the Advantage 2 PCR
105 kit (Clontech). Each RACE product was cloned in pCRII vector (Invitrogene), and at least 5
106 independent clones were sequenced. To confirm RACE results, RT-PCR products were
107 amplified using the Expand High Fidelity PCR System (Roche). The location of primer
108 sequences within the exons and the complete cDNA sequences of DsEx, Ds1 and DsIntra
109 are shown in Figure S2.

110

111 **Northern blot analysis**

112 Total RNA was extracted from brain and imaginal discs of third instar larvae using TriPure
113 Isolation Reagent (Roche). RNA was quantified in a nanodrop ND-1100. The quality of
114 each sample was checked in an Agilent 2100 bioanalyzer. For Northern blot analysis, 20 µg
115 of total RNA were loaded on 1% agarose-formaldehyde gels and run in MOPS1X buffer.
116 After RNA transfer, the nylon membranes (Roche) were hybridized at 60°C in modified
117 Church & Gilbert's hybridization buffer [23]. Detection was performed with CDP-Star
118 according to the DIG RNA Detection Protocol (Roche). The digoxigenin-labeled anti-sense
119 RNA probes were synthesized according to the same protocol. As templates, we used two
120 different cDNA fragments: one of 5.2 kb (exons 2-11; clone 119 in Clark, 1995) and the 1.4
121 kb fragment of exon12 corresponding to the coding sequence of the cytoplasmic domain.
122 The size of the bands was determined by extrapolation from a standard curve using RNA
123 molecular size markers.

124

125 **Western blot analysis**

126 For Western blot analysis, total proteins were isolated from imaginal discs and brain in
127 Ringer's solution, supplemented with complete protease inhibitor cocktail (Roche). Aliquots
128 of protein extracts (30 µg) from different genotypes were loaded and separated on 4-15%
129 Mini-PROTEAN TGX Precast Gel (BioRad) and transferred onto PVDF membranes
130 (BioRad). For detection of Ds isoforms containing the cytoplasmic region, a guinea pig anti-
131 Ds antibody (1:2000) and an anti-guinea pig HRP conjugated antibody (1:2000) were used.
132 For detection of Ds isoforms containing the extracellular region, a rabbit anti-Ds antibody
133 (1:2000) [20] and an anti-rabbit HRP conjugated antibody (1:2000) were used. Membranes
134 were developed with the ECL reagent kit.

135

136 **RESULTS**

137 **Expression of Dachshous protein in mutant imaginal discs**

138 To analyze how Ds protein is expressed in different *ds* mutant backgrounds, we
139 used two antibodies - Ds^{ex} and Ds^{cyt} - generated against the extracellular and cytoplasmic

140 region, respectively (Figure 1). To test their specificity we performed analysis of
141 immunostaining and western blotting (Figure 1B, 1C). As expected, in wild-type (wt) flies,
142 Ds expression in wing discs was similar with both antibodies and preferentially located at the
143 apical membrane of disc proper cells (Figure 1D, 1D'). However, in Western blot the pattern
144 of bands detected by Ds^{ex} and Ds^{cyt} antibodies was different (Figure 1C). Moreover, the
145 bands would correspond to proteins smaller than the reported full-length Ds protein (DsFL;
146 385 kDa) [17]. Strikingly, Ds^{cyt} antibody revealed a doublet around 50 kDa, not detected by
147 Ds^{ex}. The similar levels of these bands in DsFL and wt cells rule out that they could derive
148 from proteolytic processing of DsFL. Although the results obtained with Ds^{ex} antibody are
149 less conclusive, DsFL seems to be expressed at low levels in wt cells at larval stage. In
150 contrast, the protein detected by each antibody was different in mutant backgrounds. In
151 *ds^{38K}/ds^{36D}* discs, Ds was almost undetectable with Ds^{cyt}, whereas the protein detected by
152 Ds^{ex} was evenly distributed (Figure 1E', 1E''). Those differences became more evident in
153 *ds¹/ds¹* wing discs, in which Ds expression monitored by Ds^{cyt} looked apparently normal,
154 while Ds^{ex} revealed a speckled pattern of Ds distributed between the cytoplasm and the
155 apical membrane (Figure 1F', 1F''). Furthermore, we observed a correlation between the
156 severity of the wing defects and the lack of apical expression detected by Ds^{cyt}.

157 Therefore, the distribution of Ds and the different bands detected by each antibody
158 suggest the presence of additional isoforms other than DsFL in the imaginal discs and
159 brain.

160

161 **Quantitative real-time PCR analysis of *ds* expression**

162 To investigate this hypothesis, we performed a quantitative real-time PCR (qRT-
163 PCR) assay to analyze the expression of individual exons in wt imaginal discs and brain -
164 two tissues in which *ds* is preferentially expressed (Figure 2A; Table S1). The full-length
165 cDNA (DsFL) comprises 12 exons (Genbank: L08811.2) and the sequence was determined
166 from the assembly of overlapping clones derived from two embryonic cDNA libraries [17].
167 Exon 12 encodes the complete cytoplasmic region, the transmembrane domain and a small

168 part of the extracellular domain. Therefore, we decided to split exon12 into two fragments
169 named 12A and 12B to separately analyze the expression of the cytoplasmic region
170 comprised in 12B (Figure 2A). Absolute quantification of individual exons was determined
171 using *pUAS-dsFL* DNA as standard.

172 An overall comparison showed significant differences in expression levels among
173 individual exons (Figure 2A; Table S2). The highest level corresponded to 12B, with a 10-
174 fold increase with respect to exon2 (the lowest value). These results point out two main
175 conclusions: firstly, according to the relative expression of different exons, several
176 alternative transcriptional isoforms are expressed at this developmental stage. Secondly,
177 DsFL is expressed at lower levels than other transcripts (comparing exon2 to other exons;
178 Table S2). Moreover, difference in the expression of 12A and 12B suggests the existence of
179 novel isoforms containing the cytoplasmic region different to DsFL (exon12) [17].

180

181 **Characterization of three novel Ds isoforms**

182 To elucidate the molecular structure of putative novel transcripts, we used two
183 different approaches: Northern blot analysis and RACE assay. Up to 8 prominent bands
184 ranging from about 6.0 kb to 0.7 kb were detected with Northern blot hybridization using two
185 different RNA probes comprising either extracellular or cytoplasmic sequences (Figure 2B).
186 Again, the predicted sizes would correspond to potential cDNAs significantly shorter than
187 DsFL (12.4 kb). Strikingly, some bands were exclusively detected by one of the two probes
188 (Figure 2B; red asterisk). Under these experimental conditions we could not detect the band
189 corresponding to DsFL; however, using alkaline conditions to facilitate the transfer of higher
190 bands, a faint band similar in size to *pUAS-ds* (internal control) was detected, indicating that
191 a larger transcript is expressed at low levels (not shown).

192 Next, RACE assay was used to identify the novel cDNAs. Although specific RACE
193 primers were designed for most *ds* exons, we could only accurately determine the
194 sequence of three novel isoforms named DsEx, Ds1 and DsIntra (Figure 2C; Figure S2).
195 DsEx cDNA comprises exons 1 to 10 and might correspond to the 6.0 kb band detected by

196 Northern blot. Sequence analysis of the 3'RACE (ex10) product showed the existence of a
197 larger novel exon 10 (exon10B) ending with a stop codon followed by a well-defined
198 polyadenylation signal. This result was confirmed by RT-PCR amplification using a forward
199 primer exon1 and the reverse primer ex10.1 (Figure S2C).

200 Ds1 is a small cDNA of 2.6 kb comprising exon1 and exon2B (new 3' end at position
201 2432 in L08811.2) followed by exon12C, a short exon only containing a long
202 polyadenylation signal (11235-11360nt in L08811.2). Ds1 cDNA was determined by
203 sequence analysis of 5'RACE (ex2) and 3'RACE (ex2) products, and was confirmed by RT-
204 PCR amplification (Figure S2C). Accordingly, a band similar in size was detected with both
205 RNA probes by Northern blot (Figure 2B).

206 Unexpectedly, we identified DsIntra, a cDNA that encodes the whole cytoplasmic
207 domain without the trans-membrane domain. The 5' and 3' ends were accurately
208 determined by sequencing of 5'RACE (ex12) and 3'RACE (ex12) products amplified with
209 overlapping primers (Figure S2). The 5' untranslated sequence was followed by an ORF that
210 encodes the whole cytoplasmic domain and corresponds to a novel exon named
211 exon12B (initiator methionine at 10156 in L08811.2; Figure S2). Other RACE products were
212 ruled out after sequencing analysis because their sequences were not consistent being
213 probably incomplete RACE products.

214 Next, we checked by Western blot analysis the expression of these potential Ds
215 proteins (Figure 2D). The double band around 50 kDa, revealed by Ds^{cyt} antibody, could
216 correspond to the predicted size of the DsIntra protein (Figure 2D; red bracket). However,
217 we could not accurately determine the expression of DsEx (217 KDa) that might correspond
218 to a faint band around 220 kDa (Figure 2D; red asterisk).

219 To summarize, using different experimental approaches we have characterized
220 three novel isoforms: the cytoplasmic protein DsIntra, and the extracellular ones DsEx and
221 Ds1 that comprise 17 and 4 cadherin domains, respectively. Nonetheless, the detection of
222 additional bands by Northern and Western blot suggests the existence of other
223 uncharacterized isoforms.

224

225 **Depletion of isoforms comprising exon12B reproduces strong mutant phenotypes**

226 To investigate the functional relevance of Ds isoforms, we examined the wing
227 phenotypes generated by the overexpression of two different double-strandedRNA
228 (dsRNAi):dsRNAi-ex and dsRNAi-cyt target the exon6 (extracellular) and exon12B
229 (cytoplasmic), respectively (Figure 1A). The overexpression ofdsRNAi-cyt in the whole wing
230 (638G4) produces phenotypes similar to those observedin strong *ds* alleles (compare
231 Figures 2E and 1E), whereas the wing defects observed with dsRNAi-exare weaker and
232 resemble those observed in *ds*¹ and *30AG4* wings (compare Figure 2E and 1F; Figure S3).
233 Interestingly, the molecular lesions of weak alleles map in exons encoding the extracellular
234 region. The different behaviour of both dsRNAi might be explained by either a lower
235 efficiency of dsRNAi-exor a lesser relevance for Ds activityof the isoforms eliminated.To
236 check the interference ability of these dsRNAi, we analyzed the relative expression of
237 individual exons in two *tubG4/UAS-dsRNAi* cellsnormalized to wt expression (Figure 2F;
238 Table S3). In both cases, we observed a general decrease in the expression levels, though
239 not identical for each exon. Surprisingly, the silencing efficiency of dsRNAi-ex was higher
240 than that ofdsRNAi-cyt. In dsRNAi-ex cells, the expression of exons 8 and 10 dropped to
241 0.25similar to targeted exon6,whereas exons such as exon2 or exon9 had 2 or 3 times
242 higherexpression - supporting the existence of alternative splicing isoforms with different
243 extracellular domain. In dsRNAi-cytcells, the expression of exon12B was higher than in
244 dsRNAi-excells (Figure 2F, 2G; fragment 12S). This apparent discrepancy can be explained
245 by the Northern blot results. The presence of several small bands (< 2.3 kb) detected only
246 by the cytoplasmic probe suggests the expression of transcripts encoding only part of the
247 cytoplasmic region (Figure 2B). The transcripts not targeted bydsRNAi-cytcould be quantified
248 by qRT-PCR. Consistently, exon12B expression was undetectable using anotherprimer pair
249 to amplify the whole cytoplasmic domain (fragment 12L) (Figure 2H).

250 Thus, we conclude that several *ds* transcriptional isoforms are expressed in imaginal
251 discs and brain. These transcripts would encode proteins comprising different extracellular

252 or cytoplasmic domains. Moreover, the isoforms eliminated by dsRNAi-cytxpression play
253 an important role in the regulation of PCP/patterning and growth.

254

255 **Ds is required for mitochondrial function**

256 Recently, it has been reported a novel role of Ft protein regulating mitochondria
257 activity through a C-terminal proteolytic peptide (Ft^{Mito}) imported into the mitochondrion after
258 cleavage of the large transmembrane protein Ft [24]. Ft^{Mito} regulates oxidative
259 phosphorylation. Above, we have shown the importance of the cytoplasmic domain for Ds
260 activity and the expression of Ds^{Intra} isoform during larval development. To investigate
261 whether Ds is also required for mitochondrial function, first we examined the expression of
262 Ds with Ds^{ex} and Ds^{cyt} antibodies in fat body cells using COXIV antibody as specific marker
263 for mitochondria (Figure 3). In wt cells, Ds only detected by Ds^{cyt} antibody colocalizes with
264 COXIV indicating that Ds is localized in the mitochondria (Figure 3A). Conversely, in *ds*
265 mutant cells, COXIV staining is decreased and the number and size of mitochondria is
266 altered compared to wt cells (Figure 3B). Surprisingly, we observed that Ds isoforms
267 detected by Ds^{ex} are now accumulated in the nuclei.

268 Next, we examined mitochondrial activity in *ds* mutant cells, analyzing the
269 accumulation of ROS (reactive oxygen species) in wing discs as detected by
270 dihydroethidium (DHE) (Figure 3C). In dsRNAi-cyt cells, DHE staining is drastically
271 increased compared to wt cells. A consequence of mitochondrial dysfunction is the
272 activation of JNK signaling induced by ROS [25]. Accordingly, in dsRNAi-cyt cells we also
273 observed upregulation of *puckered* (*puc*) gene, a target and functional read out of
274 JNK signaling and activation of Caspase 3 (Figure 3D, 3E). In contrast, the expression of
275 these targets is unaffected in dsRNAi-ex expressing-cells (Figure 3F, 3G). Overexpression of
276 Ds^{Intra} in P cells results in a smaller P compartment but does not affect the activity of JNK
277 signalling (Figure 3H).

278 These results show a novel function of Ds in the mitochondria. Ds is required for
279 proper mitochondrial morphology, and the depletion of Ds isoforms containing the

280 cytoplasmic domain promotes elevated levels of ROS and JNK signaling indicating that Ds
281 modulates the activity of the mitochondrial electron transport machinery.

282

283 **DsIntra contributes to regulate PCP/patterning and growth**

284 The function of the extracellular and cytoplasmic domains of Ds in growth and
285 PCP/patterning has been approached by miss-expression of truncated forms derived from
286 DsFL [14, 15]. These Ds forms consist of proteins anchored to the cell membrane and
287 lacking either the extracellular or the cytoplasmic domains.

288 To assess the function of DsEx and DsIntra in the regulation of PCP/patterning and
289 growth, we made two transgenes with a C-terminal tag: DsIntraV5 and DsExGFP. The wing
290 phenotypes caused by the overexpression of these Ds isoforms were compared (Figure 4).
291 Furthermore, we quantified their contribution to PCP/patterning and growth by analyzing
292 two different parameters: the A-PCV distance and the relative wing area. To measure wing
293 area variations the transgenes were overexpressed in P cells (hhG4) (Figure 4D-4M; Figure
294 S1).

295 The wing phenotype of DsIntra and DsFL was similar, indicating that the cytoplasmic
296 domain is sufficient to reproduce the dominant negative phenotype observed in DsFL wings
297 (Figure 4A, 4B, 4D, 4E, 4I, 4J). Indeed, DsIntra and DsFL wings exhibited abnormal polarity
298 (proximal), were smaller and the cross-veins distance was shorter. In contrast, DsEx
299 overexpression did not cause any obvious alteration, the wings looked apparently normal
300 and the hairs orientation was unaffected (Figure 4C, 4F, 4K). To test the ability of DsIntra
301 and DsEx to rescue growth alterations, both were expressed in the P compartment (hhG4)
302 of *ds^{38K}/ds^{36D}* flies. Unfortunately, DsIntra and DsFL overexpression, consistent with the
303 dominant negative effect, increased lethality at the early pupal stage (> 95%), and only a
304 few adult flies emerged (unfolded wings with more severe alterations). Conversely, DsEx
305 overexpression increased the viability of adult mutant flies without any obvious wing rescue.

306 Finally, we analyzed how DsIntra and DsEx overexpression affects the activity of
307 Hippo pathway by monitoring the expression of *dally-like (dlp)* [8] (Figure 4N-4P). Similar to

308 DsFL, the expression of DsIntra in the P cells(hhG4) leads to downregulation of Dlp
309 expression, whereas DsEx did not cause any detectable change. We also examined Dlp
310 expression in wing discs overexpressing dsRNAi-ex and dsRNAi-cyt (Figures 4Q, 4R). In
311 accordance with the growth defects observed in the wing, dsRNAi-cyt caused an
312 upregulation of Dlp in P cells (Figure 4R). Strikingly, in dsRNAi-ex cells Dlp expression was
313 almost eliminated suggesting an increased Hippo activity (Figure 4Q).

314 These results show that different Ds isoforms contribute to the regulation of
315 PCP/patterning and growth by modulating the activity of the Hippo pathway. Moreover, the
316 opposite effect in Dlp levels observed in dsRNAi-ex and dsRNAi-cyt cells would suggest that
317 certain Ds isoforms could act by repressing the Hippo activity.

318

319 **DISCUSSION**

320 The reported *ds* cDNA was derived from an embryonic library, and encodes a
321 single-pass transmembrane cadherin (DsFL) with a large extracellular domain and a small
322 cytoplasmic domain [17]. DsFL is preferentially localized at the apical membrane [18, 20].
323 However, reported results such as the upregulation of *dlp* expression within the clone of *ds*
324 mutant cells [8] or the inability of ectoDs expression to reverse the hairs polarity in a *ds*
325 mutant background [15] indicate a cell-autonomous mechanism of Ds difficult to envision
326 through the interaction of Ds extracellular domain with Ft, as proposed in the current model.

327 In this work, using several molecular techniques, we have detected the expression of
328 different *ds* transcriptional isoforms that reveal a complex regulation of the *ds* gene in larval
329 development. We have characterized three novel transcripts that encode the soluble
330 proteins DsEx, Ds1 and DsIntra. Furthermore, qRT-PCR and Western blot data indicate
331 that DsFL is in fact less abundant than other isoforms expressed at this developmental
332 stage. The detection of additional bands by Northern blot and RACE assays suggest the
333 expression of additional isoforms not yet characterized. In addition, the sequence analysis
334 has revealed the existence of exons not previously described such as exon2B, exon10B,
335 exon12B and exon12C. We confirmed by Western blot the expression of DsIntra protein.

336 The similar levels observed in wt and DsFL expressing-cells rule out the possibility that
337 DsIntra is a peptide derived by proteolytic cleavage of DsFL as it was suggested to explain
338 the existence of small bands detected by Ds^{cyt} antibody [26].

339 A genetic analysis derived from the expression of different Ds isoforms and two
340 specific RNAi has confirmed the functional relevance of the cytoplasmic domain in the
341 regulation of PCP/patterning and growth. Indeed, there is a clear correlation between the
342 severity of the wing defects and the absence of isoforms comprising the cytoplasmic
343 domain monitored at protein (Ds^{cyt}) and RNA (qRT-PCR) levels. Consistently, two proteins
344 that control the Hippo activity such as Riquiqui and Minibrain interact physically with Ds
345 cytoplasmic domain [27]. Although we cannot assign specific functions to individual
346 isoforms, the existence of DsIntra can help to understand the cell-autonomous regulation by
347 Ds of PCP/patterning and growth. However, the new role of Ds in mitochondrial activity
348 further supports the importance of the cytoplasmic domain in the mechanism of action of
349 Ds. Furthermore, the wings phenotypes observed in *ds*¹ and dsRNAi-ex flies indicate that
350 isoforms comprising an extracellular domain also participate in the regulation of growth.
351 Interestingly, the expression of Dlp in dsRNAi-ex cells would suggest that some isoforms
352 could negatively modulate Hippo activity.

353 In vertebrates, distinct transcriptional isoforms of cadherin-related proteins such as
354 CDH23 and PCDH15 are expressed in different tissues. Also, alternative splice variants of
355 FAT1 have been reported in mouse although the complete cDNAs have not been
356 determined [28]. Therefore, since all these proteins are main components of the
357 PCP signaling cascade [29, 30], this suggests that the existence of isoforms might be
358 an evolutionary conserved mechanism used by these genes to provide different cellular
359 responses during development [31].

360 Given that *ds* expression pattern is very dynamic along development, the next
361 challenge will be to determine how its isoforms are spatial- and temporally regulated, in
362 order to understand how Ds activity can regulate processes such as PCP, patterning, cell

363 proliferation, mitochondrial activity or even other still unknown. The combination of Ds
364 isoforms in each developmental context could determine the cellular response.

365

366 **ACKNOWLEDGEMENTS**

367 We thank S. Campuzano, M. Dominguez, and C. Cobaleda for insightful comments and
368 critical reading of the manuscript. We also thank M. Gomez and A. Mudarra for advice and
369 help with the qRT-PCR experiments and data analysis. To the Bloomington Stock Center
370 and Drosophila RNAi Center (VDRC) for Drosophila stocks. To D. Strutt and the
371 Developmental Studies Hybridoma Bank for antibodies. E.R. is a Research Fellow of Word
372 Works Science. This research was supported by project grants BFU2008-01869 and
373 BFU2011-22617 from the DGICYT, and an institutional grant from Fundación Ramón
374 Areces for the CBMSO.

375

376 **REFERENCES**

- 377 1. Goodrich, L.V., and Strutt, D. (2011). Principles of planar polarity in animal
378 development. *Development* 138, 1877-1892.
- 379 2. Thomas, C., and Strutt, D. (2011). The roles of the cadherins Fat and Dachshous in
380 planar polarity specification in Drosophila. *Dev Dyn*.
- 381 3. Harumoto, T., Ito, M., Shimada, Y., Kobayashi, T.J., Ueda, H.R., Lu, B., and
382 Uemura, T. (2010). Atypical cadherins Dachshous and Fat control dynamics of
383 noncentrosomal microtubules in planar cell polarity. *Dev Cell* 19, 389-401.
- 384 4. Baena-Lopez, L.A., Baonza, A., and Garcia-Bellido, A. (2005). The orientation of cell
385 divisions determines the shape of Drosophila organs. *Curr Biol* 15, 1640-1644.
- 386 5. Rodriguez, I. (2004). The dachshous gene, a member of the cadherin family, is
387 required for Wg-dependent pattern formation in the Drosophila wing disc.
388 *Development* 131, 3195-3206.
- 389 6. Adler, P.N., Charlton, J., and Liu, J. (1998). Mutations in the cadherin superfamily
390 member gene dachshous cause a tissue polarity phenotype by altering frizzled
391 signaling. *Development* 125, 959-968.
- 392 7. Willecke, M., Hamaratoglu, F., Sansores-Garcia, L., Tao, C., and Halder, G. (2008).
393 Boundaries of Dachshous Cadherin activity modulate the Hippo signaling pathway to
394 induce cell proliferation. *Proc Natl Acad Sci U S A* 105, 14897-14902.
- 395 8. Baena-Lopez, L.A., Rodriguez, I., and Baonza, A. (2008). The tumor suppressor
396 genes dachshous and fat modulate different signalling pathways by regulating dally
397 and dally-like. *Proc Natl Acad Sci U S A* 105, 9645-9650.
- 398 9. Rodriguez, I., Baena-Lopez, L.A., and Baonza, A. (2008). Upregulation of glypicans
399 in Hippo mutants alters the coordinated activity of morphogens. *Fly (Austin)* 2, 320-
400 322.
- 401 10. Matakatsu, H., and Blair, S.S. (2012). Separating planar cell polarity and Hippo
402 pathway activities of the protocadherins Fat and Dachshous. *Development* 139,
403 1498-1508.

- 404 11. Pan, G., Feng, Y., Ambegaonkar, A.A., Sun, G., Huff, M., Rauskolb, C., and Irvine,
405 K.D. (2013). Signal transduction by the Fat cytoplasmic domain. *Development* 140,
406 831-842.
- 407 12. Matis, M., and Axelrod, J.D. (2013). Regulation of PCP by the Fat signaling
408 pathway. *Genes Dev* 27, 2207-2220.
- 409 13. Staley, B.K., and Irvine, K.D. (2012). Hippo signaling in *Drosophila*: recent advances
410 and insights. *Dev Dyn* 241, 3-15.
- 411 14. Matakatsu, H., and Blair, S.S. (2006). Separating the adhesive and signaling
412 functions of the Fat and Dachshous protocadherins. *Development* 133, 2315-2324.
- 413 15. Casal, J., Lawrence, P.A., and Struhl, G. (2006). Two separate molecular systems,
414 Dachshous/Fat and Starry night/Frizzled, act independently to confer planar cell
415 polarity. *Development* 133, 4561-4572.
- 416 16. Martin-Blanco, E., Gampel, A., Ring, J., Virdee, K., Kirov, N., Tolkovsky, A.M., and
417 Martinez-Arias, A. (1998). puckered encodes a phosphatase that mediates a
418 feedback loop regulating JNK activity during dorsal closure in *Drosophila*. *Genes*
419 *Dev* 12, 557-570.
- 420 17. Clark, H.F., Brentrup, D., Schneitz, K., Bieber, A., Goodman, C., and Noll, M.
421 (1995). Dachshous encodes a member of the cadherin superfamily that controls
422 imaginal disc morphogenesis in *Drosophila*. *Genes Dev* 9, 1530-1542.
- 423 18. Matakatsu, H., and Blair, S.S. (2004). Interactions between Fat and Dachshous and
424 the regulation of planar cell polarity in the *Drosophila* wing. *Development* 131, 3785-
425 3794.
- 426 19. Gomez-Skarmeta, J.L., Rodriguez, I., Martinez, C., Culi, J., Ferres-Marco, D.,
427 Beamonte, D., and Modolell, J. (1995). Cis-regulation of achaete and scute: shared
428 enhancer-like elements drive their coexpression in proneural clusters of the imaginal
429 discs. *Genes Dev* 9, 1869-1882.
- 430 20. Strutt, H., and Strutt, D. (2002). Nonautonomous planar polarity patterning in
431 *Drosophila*: dishevelled-independent functions of frizzled. *Dev Cell* 3, 851-863.
- 432 21. Baltzer, C., Tiefenbock, S.K., Marti, M., and Frei, C. (2009). Nutrition controls
433 mitochondrial biogenesis in the *Drosophila* adipose tissue through Delg and cyclin
434 D/Cdk4. *PLoS One* 4, e6935.
- 435 22. Owusu-Ansah, E., Yavari, A. and Banerjee, U. (Published online 27 February 2008).
436 A protocol for in vivo detection of reactive oxygen species. *Protocol Exchange*.
- 437 23. Church, G.M., and Gilbert, W. (1984). Genomic sequencing. *Proc Natl Acad Sci U S*
438 *A* 81, 1991-1995.
- 439 24. Sing, A., Tsatskis, Y., Fabian, L., Hester, I., Rosenfeld, R., Serricchio, M., Yau, N.,
440 Bietenhader, M., Shanbhag, R., Jurisicova, A., et al. (2014). The atypical cadherin
441 fat directly regulates mitochondrial function and metabolic state. *Cell* 158, 1293-
442 1308.
- 443 25. Chambers, J.W., and LoGrasso, P.V. (2011). Mitochondrial c-Jun N-terminal kinase
444 (JNK) signaling initiates physiological changes resulting in amplification of reactive
445 oxygen species generation. *The Journal of biological chemistry* 286, 16052-16062.
- 446 26. Ambegaonkar, A.A., Pan, G., Mani, M., Feng, Y., and Irvine, K.D. (2012).
447 Propagation of Dachshous-Fat planar cell polarity. *Curr Biol* 22, 1302-1308.
- 448 27. Degoutin, J.L., Milton, C.C., Yu, E., Tipping, M., Bosveld, F., Yang, L., Bellaiche, Y.,
449 Veraksa, A., and Harvey, K.F. (2013). Riquiqui and minibrain are regulators of the
450 hippo pathway downstream of Dachshous. *Nat Cell Biol* 15, 1176-1185.
- 451 28. Braun, G.S., Kretzler, M., Heider, T., Floege, J., Holzman, L.B., Kriz, W., and
452 Moeller, M.J. (2007). Differentially spliced isoforms of FAT1 are asymmetrically
453 distributed within migrating cells. *The Journal of biological chemistry* 282, 22823-
454 22833.
- 455 29. Webb, S.W., Grillet, N., Andrade, L.R., Xiong, W., Swarthout, L., Della Santina,
456 C.C., Kachar, B., and Muller, U. (2011). Regulation of PCDH15 function in
457 mechanosensory hair cells by alternative splicing of the cytoplasmic domain.
458 *Development* 138, 1607-1617.

459 **FIGURE LEGENDS**

460 **Figure 1. Distribution of Ds Protein in different mutant backgrounds.**

461 A) Schematic drawing of the *dachsous* gene shows the molecular lesion and location of *ds*
462 alleles (red). The exons (blue boxes) correspond to the cDNA that encodes DsFL
463 protein, composed of an extracellular region with 27 cadherin domains (brown circles), a
464 transmembrane domain (TM; black) and a small cytoplasmic region (cyt; blue line). B)
465 Expression of Ds protein in imaginal wing discs to show the specificity of Ds^{ex} and Ds^{cyt}
466 antibodies. DsFL protein is detected in the P compartment by both antibodies whereas
467 ectoDs form is only detected by Ds^{ex} antibody. A clone of *ds* mutant cells is marked by the
468 absence of GFP. C) Western blot analyses of cell lysates from wt, tubG4>UAS-ectoDs and
469 tubG4>UAS-DsFL imaginal discs and brains. A double-band around 50 kD detected with
470 Ds^{cyt} antibody is expressed at the same level in DsFL and wt cells (red bracket); however the
471 lower band is eliminated in ectoDs cells suggesting a potential crossregulation between
472 isoforms. An extra band around 40 kD is detected when ectoDs and DsFL are
473 overexpressed. D-F) Adult wings and higher-magnification of the wing proximal region of D)
474 wild type (wt), E) *ds^{38k}/ds^{36D}* and F) *ds¹/ds¹* flies. The impairment of Ds activity can be
475 visualized as smaller and rounded wings, defective vein pattern and a swirling pattern of
476 hairs. XY view and Z-section (white line) of wing discs stained with Ds^{ex} (green) and Ds^{cyt}
477 (red) antibodies. D'') In wt cells, Ds protein is preferentially detected at the apical
478 membrane. E'') In *ds^{38k}/ds^{36D}* discs (strong alleles), Ds is delocalized and evenly distributed
479 monitored by Ds^{ex} antibody and almost undetectable with Ds^{cyt}. F'') In *ds¹/ds¹* discs (weak
480 allele), note the different distribution of Ds protein detected with Ds^{ex} and Ds^{cyt}. Cells were
481 visualized by Phalloidin staining (Pha). Abbreviations: A anterior ; P posterior

482

483 **Figure 2. Characterization of novel Ds isoforms.** A) qRT-PCR analysis showed high
484 variability in the expression of individual exons in wt cells. 12B: cDNA fragment encoding
485 the cytoplasmic domain. B) Northern blot analysis of total RNA from wild-type cells revealed
486 by two RNA probes. Bands detected only by one of the probes are indicated (red

487 asterisk).C) Schematic illustration of three novel Ds isoforms. The cDNA and the predicted
488 proteins are shown for each isoforms. Brown boxes: novel exons described in this work. D)
489 Cell lysates from tubG4>UAS-DsIntra cells indicate that the double-band ~50kD would
490 correspond to the DsIntra isoform. E)Adult wings of flies expressing two different dsRNAi in
491 the entire wing (638G4). dsRNAi-cyt wings resemble defects observed in strong ds alleles.
492 dsRNAi-ex expression causes mild defects. (F-H) qRT-PCR analysis of individual exons in
493 tubG4>UAS-dsRNAi-ex and tubG4>UAS-dsRNAi-cyt cells. The interference ability of
494 dsRNAi-ex is higher than that of dsRNAi-cyt. (G, H) Exon12B expression in dsRNAi-cyt
495 cells using two different primerpair (12S and 12L: PCR fragments amplified). dsRNAi-cyt
496 expression eliminates the isoforms comprising the whole cytoplasmic domain. Bars show
497 the mean \pm SD. * $p < 0.05$, ** $p < 0.01$, *** $p < 0.001$.

498

499 **Figure 3.Ds control mitochondrial activity in the larval fat body.**

500 (A,B)Ds expression in fat body cells of third instar larvae. The mitochondria and nuclei were
501 visualized with COXIV (green spots) and DAPI (pink) respectively. A) In wt cells Ds^{cyt}
502 staining is prominent in the mitochondria marked with COXIV antibody. Dsex staining is not
503 detected. B) In *ds^{38K}* the fat body cell morphology is altered and the size and number of
504 mitochondria is reduced. Strikingly, in these mutant cells Ds expression is almost
505 undetectable with Ds^{cyt} and Ds^{ex} staining colocalizes with DAPI indicating the
506 abnormal expression of Ds isoforms with extracellular domain in the nuclei. C) In
507 enG4>UASdsRNAi-cyt wing discs, the mutant territory (P cells) shows elevated ROS levels
508 compared to wt cells (A cells) detected by DHE staining.(D-H) Activity of JNK pathway in
509 enG4>UASdsRNAi-ex, enG4>UASdsRNAi-cyt and enG4>UASDsIntra can be observed by
510 monitoring two downstream targets such as pucZ and Cas3. Depletion of Ds isoforms
511 containing the cytoplasmic domain (dsRNAi-cyt) results in a clear upregulation of *pucZ*
512 expression and increased cell-death detected with Cas3. However, neither the expression of
513 dsRNAi-ex nor DsIntra caused any change in the expression of these targets. The

514 expression of pucZ and Cas3 are shown as an independent panel in grey. Abbreviations: A
515 anterior ; P posterior

516

517 **Figure 4. Contribution of different Ds isoforms to the control of PCP/Patterning and**
518 **growth.** Adult wings of flies overexpressing the following transgenes: (A,D) UAS-DsFL,
519 (B,E) UAS-DsIntraV5 and (C,F) UAS-DsExGFP in the entire wing (638G4) and the P
520 compartment (hhG4). (G,H) Adult wings of flies overexpressing dsRNA_{iex} and dsRNA_{icyt} in
521 P cells (hhG4). (I-M) Average of A-PCV distance and wing area of flies expressing DsFL,
522 DsIntra, DsEx, dsRNA_{icyt} and dsRNA_{iex} under the control of 638G4 and hhG4 respectively
523 and normalized to the value of control females. Bars show the mean \pm SD. * $p < 0.05$; ** $p <$
524 0.01 ; *** $p < 0.001$, ns: not significant. (N-R) Analysis of Hippo pathway activity in wing
525 imaginal discs expressing different transgenes in the P cells (hhG4) was monitored by the
526 expression of Dlp. (Q) In wing discs, the overexpression of dsRNA_{i-cyt} produced an
527 enlarged mutant territory, whereas (R) in dsRNA_{i-ex} wing discs P compartment was
528 significantly smaller respect to A compartment. The expression of Dlp (grey) is shown as an
529 independent panel.

530

531 **AUTHOR CONTRIBUTIONS**

532 E.R.-Y. performed the qRT-PCR and genetic experiments and analyzed the data. L.V.
533 performed RNA experiments, conducted the confocal imaging and generated Ds antibody.
534 J.S. performed protein experiments and analyzed data from the sequencing and RACE
535 assays. I.R. designed and supervised experiments, analyzed data and wrote the paper. All
536 authors discussed the results and contributed extensively to the work presented in this
537 paper. All authors gave final approval for publication.

538

539

540

541

542 **DATA ACCESSIBILITY**

543 The datasets supporting this article have been uploaded as part of the Supplementary
544 Material.

545

546

547 **COMPETING INTERESTS**

548 The authors have no competing interests.

Figure 1
[Click here to download high resolution image](#)

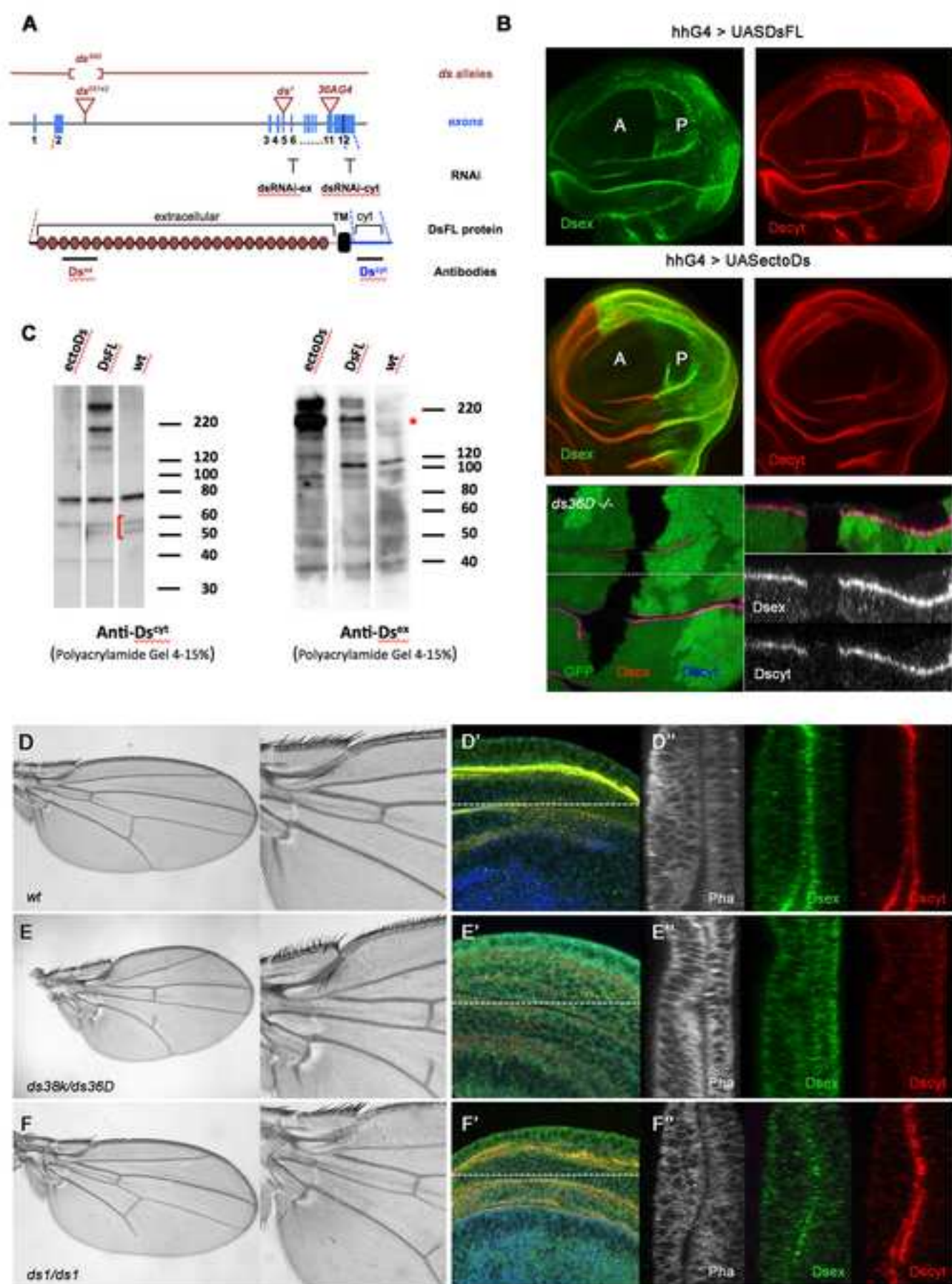


FIGURE 1

Figure 2
[Click here to download high resolution image](#)

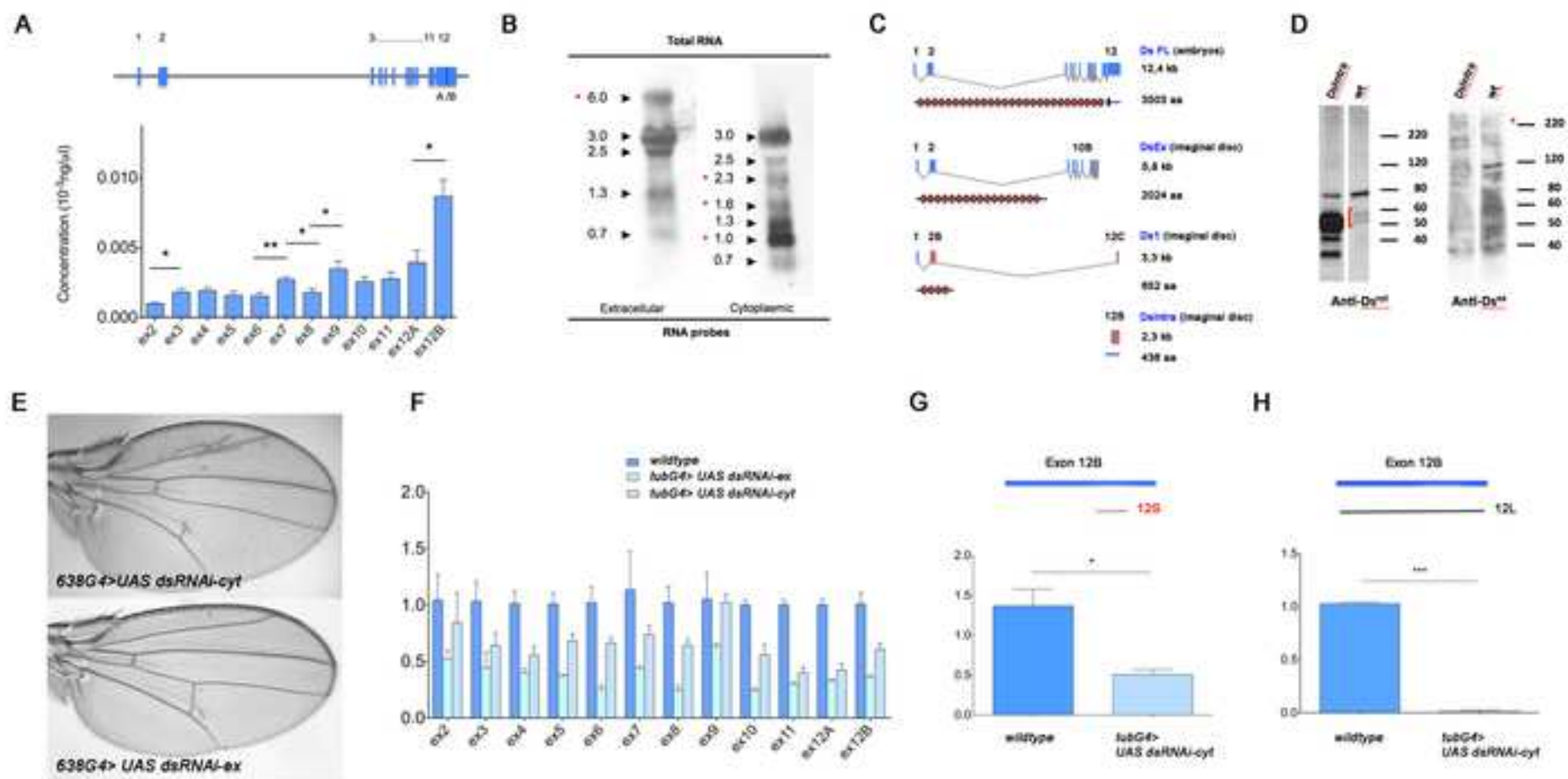


FIGURE 2

Figure 3
[Click here to download high resolution image](#)

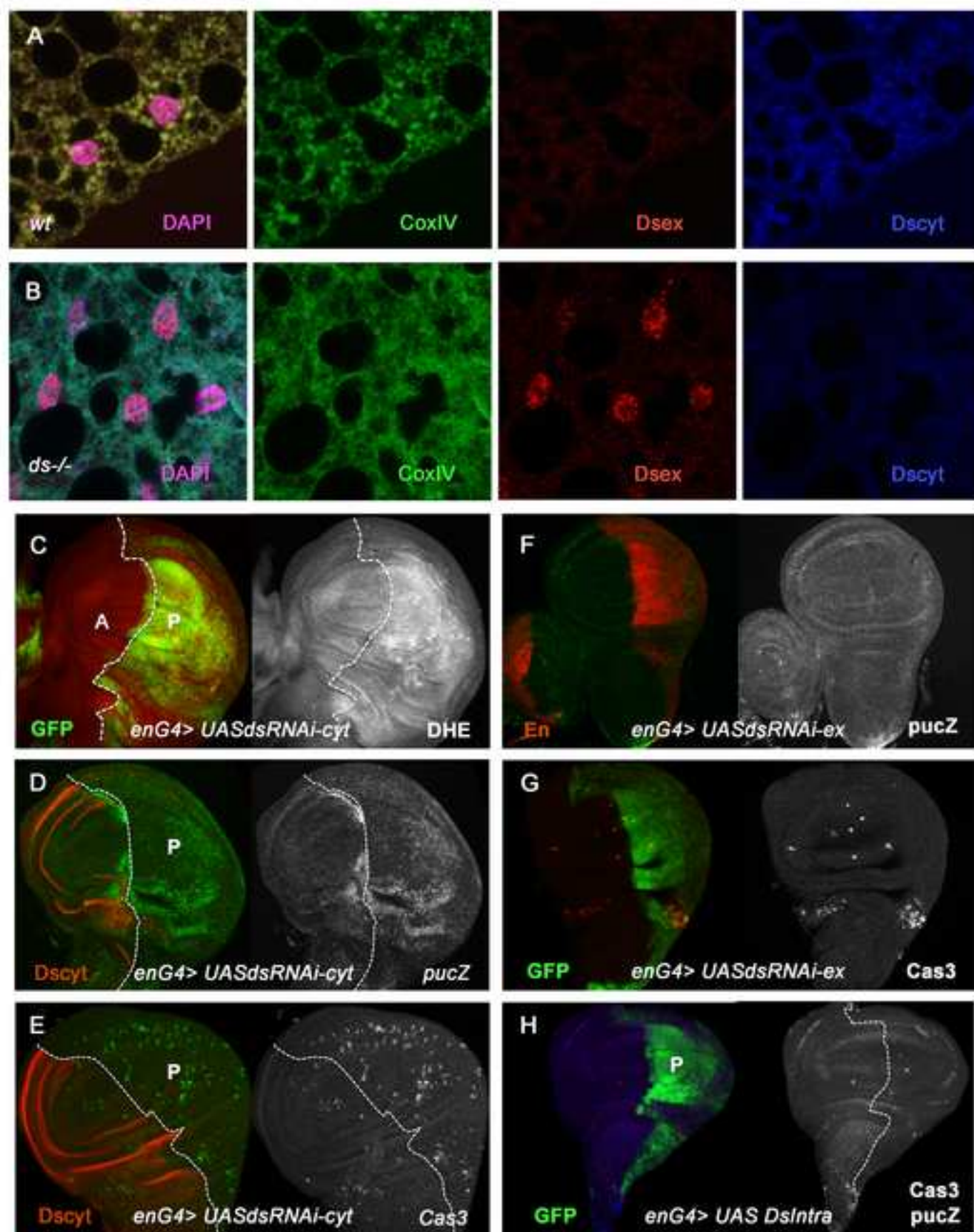


FIGURE 3

Figure 4
[Click here to download high resolution image](#)

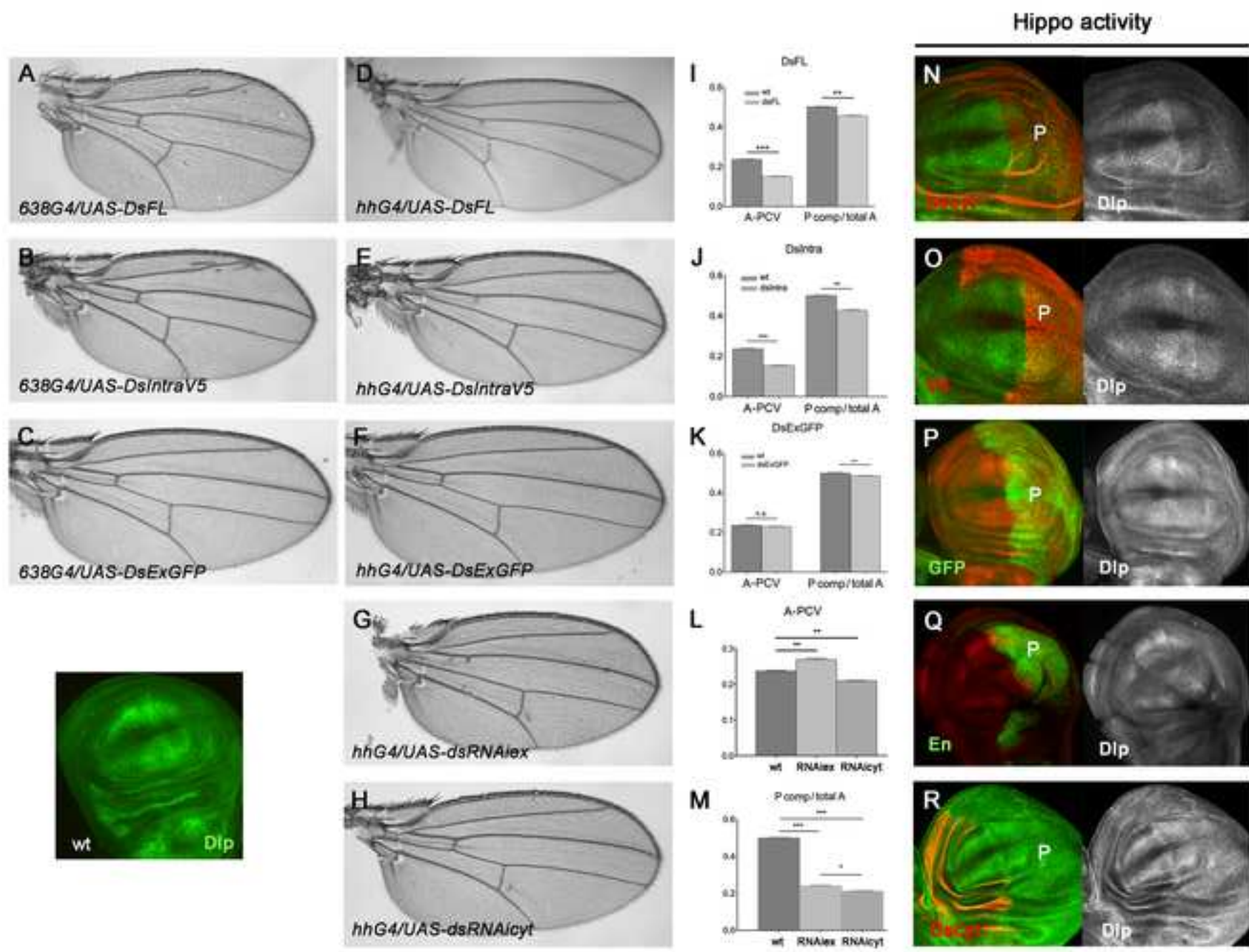


FIGURE 4

Supplementary material for online publication only

[Click here to download Supplementary material for online publication only: Supplementary Material.pdf](#)

1 **AUTHOR CONTRIBUTIONS**

2 E.R.-Y. performed the qRT-PCR and genetic experiments and analyzed the data. L.V.
3 performed RNA experiments, conducted the confocal imaging and generated Ds antibody.
4 J.S. performed protein experiments and analyzed data from the sequencing and RACE
5 assays. I.R. designed and supervised experiments, analyzed data and wrote the paper. All
6 authors discussed the results and contributed extensively to the work presented in this
7 paper. All authors gave final approval for publication.